Submonolayer growth of Fe on a GaAs(100)-2×6 reconstructed surface

A. Ionescu, M. Tselepi, D. M. Gillingham, G. Wastlbauer, S. J. Steinmüller, H. E. Beere, D. A. Ritchie, and J. A. C. Bland*
Cavendish Laboratory, University of Cambridge, Madingley Road, Cambridge CB3 0HE, United Kingdom
(Received 17 May 2004; revised manuscript received 16 June 2005; published 1 September 2005)

We present the results of *in situ* STM measurements of the submonolayer growth of Fe on the Ga-rich and As-terminated (2×6) reconstruction of the GaAs(100) surface. In the beginning of the nucleation regime (0.1 ML), the surface reconstruction influences the nucleation sites, so that almost round islands are observed solely on the top of the As rows. In the growth regime from 0.3 to 0.6 ML the islands become elliptically elongated along the [011] direction due to faster diffusion of Fe atoms along the As rows. Throughout our study, Fe atom loss is observed, becoming more pronounced from 0.6 ML onwards, due to the penetration of Fe into the substrate. This penetration leads to a trapping mechanism, which not only changes the diffusion properties of Fe clusters but also supplies extra energy to adatoms atop the Fe islands to surmount the Schwoebel barrier, resulting in a two-dimensional island nucleation from 0.3 ML onwards. A structural nucleation model is presented which provides insight into the interface structure and intermixing in the submonolayer regime.

DOI: 10.1103/PhysRevB.72.125404 PACS number(s): 68.37.Ef, 68.55.Ac, 68.55.Jk, 75.70.Ak

I. INTRODUCTION

Much current research on thin magnetic films is focusing on Fe on GaAs, one of the most studied systems since the first report of epitaxial growth of Fe on GaAs(100) by Waldrop *et al.*[1] in 1979. The interest is mainly being spurred by the need to integrate magnetic materials into semiconductor-based electronics (appropriately named spintronics). Spintronic devices such as the spin-polarized light emitting diode[2,3] or the spin-polarized field effect transistor[4,5] depend on efficient spin injection through the ferromagnet (FM) and semiconductor (SC) interface at room temperature (RT). Fe is an attractive candidate as a source of spin-polarized current at room temperature for such devices because of its high Curie temperature $T_C = 1040.2$ K.[6,7] The mode of transport of electrons propagating across the interface, i.e., diffusive, ballistic, or tunneling transport, determines the spin transmission across the interface. Recently, Schmidt *et al.*[8,9] suggested that fundamental restrictions exist for spin injection through such heterostructures in the diffusive regime which arise from the idealized metal-SC conductivity mismatch, and which typically limit the spin injection efficiency to 1% or less. However, the Schottky barrier formed between Fe and doped GaAs may provide an intrinsic tunnel barrier as an alternative to an additional tunnel barrier (e.g., Al_2O_3) to circumvent the problems of conductance mismatch.[10] The interface electronic and physical structure is therefore crucial in this context.

Over the last three decades a huge number of publications have been written concerning the growth[11–14] and magnetic[15–24] properties of Fe on GaAs(100). Earlier studies focused on the origin of a predominantly in-plane uniaxial magnetic anisotropy (UMA) with the [011] direction, the easy axis, for thicknesses up to ≈55 ML.[18,25] Krebs *et al.*[15] suggested that the dangling bond orientation, which differs by 90° according to whether an As- or Ga-terminated surface is used, might be responsible for the observed [011] vs $[0\bar{1}1]$ inequivalence. This was disproved by the realisation that the direction of the easy axis is common for all the different surface reconstructions whether As- or Ga-terminated.[13,14,22,23] Freeland *et al.*[26] suggested that the similarity of the magnetic properties on a variety of reconstructions shows that the magnetic properties are principally influenced by a common type of interface bonding, possibly connected to the strong Fe-As local bonding configuration. This suggestion is supported by the results of Wastlbauer,[23] who shows that the UMA of Fe on III-V semiconductors is related to the interplay of strain and interface bonding. For Fe/GaAs(100) the strain is almost negligible and interface bonding is the dominant contribution. Even in the first report of epitaxial growth of Fe on GaAs(100) at RT,[1] the authors indicate the tendency of the GaAs to dissociate at the interface, followed by a migration of As through the Fe layers. Growth at elevated temperatures ranging from 150–225 °C leads to enhanced interdiffusion of Fe into GaAs,[11–13,15,25,27] as one would expect from increasing atom mobility. This has been confirmed by several authors by means of Auger-electron spectroscopy (AES) or x-ray photoemission spectroscopy (XPS),[1,12,13,15,28] showing Ga and As in solution in the bcc Fe lattice and surface segregation of As on the surface of the Fe layer. Moreover, the formation of FeAs and FeGa compounds such as the nonmagnetic $FeAs_2$ and ferromagnetic $Fe_3Ga_{2-x}As_x$ in the vicinity of the interface has been shown to result in reduced or even zero magnetic moment of the Fe film there, so-called magnetically "dead" layers. It is now well established that growing the Fe film at RT (Refs. 16, 17, and 19) or even at very low temperatures [$T \approx -110$ °C (Ref. 29)] reduces the interdiffusion and interface roughness. Another possible method of reducing the interdiffusion, e.g., the segregation of As to the surface is to grow the Fe films on Ga-rich surfaces.[16,30,31] Despite the importance of the interface quality and its influence on the magnetic properties of thin films, the only extensive study of the nucleation regime of the Fe/GaAs(100) system was performed by Thibado *et al.*[11–13] for the As-rich $c(4\times4)$ and (2×4) reconstructions. Our present study aims to investigate the nucleation of Fe on a Ga-rich surface at RT, which is expected to have a reduced interdiffusion compared to the As-rich surfaces. Furthermore, the understanding of the morphological and magnetic interface properties is of para-

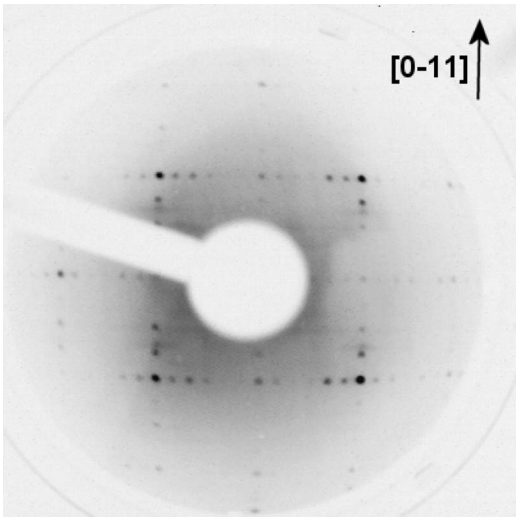

FIG. 1. LEED pattern of a "pseudo" (4×6) reconstructed GaAs (100) surface, $E=120$ eV. The "pseudo" (4×6) reconstruction pattern is clearly visible. In addition to the $4\times$ spots in the $[0\bar{1}1]$ direction some disorder lines, the so-called $2\times/3\times$ intermediate streaks, are also visible.

mount importance for spin injection, which is purely an interface effect.

II. EXPERIMENTAL METHOD

These measurements were carried out *in situ* in a "multiple technique" molecular beam epitaxy (MTMBE) chamber combining a low energy electron diffraction (LEED) and a Burleigh ultrahigh vacuum (UHV), scanning tunnelling microscope (STM) setup with a base pressure of 2.0×10^{-10} mbar. A commercial Si *n*-doped GaAs(100) wafer ($n=10^{18}$ cm^{-3}) used during these experiments had been prepared in a UHV MBE chamber beforehand. A buffer layer ($t\approx0.5$ μm) of homoepitaxial GaAs was grown on the wafer to provide an as smooth as possible surface and subsequently As capped. After transferring a 10×10 mm^2 sample to the MTMBE chamber, the As cap was removed by annealing at $T\approx400$ °C for 15 min. Afterwards, the temperature was increased to $T\approx550$ °C and maintained there for another 30 min to obtain a clean and ordered surface before the Fe growth. This treatment leads to a "pseudo" (4×6) reconstructed GaAs surface,[14,27,32–36] discussed later.

The Fe was deposited using an *e*-beam evaporator at RT with a constant rate of 0.3 ML/min. The definition of 1 monolayer (ML) of Fe (Refs. 11 and 13) is 1.216×10^{15} atoms/cm^2. The deposition was monitored with the help of a quartz microbalance. The surface reconstruction of the substrate was examined with a VG rear view LEED system. The Burleigh UHV STM was run in constant current mode with a dc etched tungsten tip. The STM images were acquired with currents in the range of 0.5 to 2.7 nA and sample biases from −1.1 to 2.8 V depending on the thickness of the Fe layer. The average Fe island sizes and areas were determined for all coverages by solving the directionally dependent Gaussian width of the 2D height-height autocorrelation function for a certain amount of images (not all shown here) and image sizes as well as for their derivatives. The results of the autocorrelation function were double checked manually by measuring randomly chosen islands on several images and evaluating these results statistically. The latter procedure was also used to determine the island height and density.

III. RESULTS

A LEED image of the GaAs substrate surface before the Fe growth is presented in Fig. 1. The pattern suggests a "pseudo" (4×6) reconstruction as observed previously by several other groups[14,32–36] for annealing temperatures of $T\approx550$ °C. The LEED pattern shows sharp $6\times$ reconstruction spots in the $[011]$ direction and additional diffuse $4\times$ spots with $2\times$ and $3\times$ intermediate streaks along the $[0\bar{1}1]$ axis. Due to this pattern, also visible with reflection high-energy electron diffraction, the surface reconstruction can be easily misinterpreted to be the high-temperature "genuine" single (4×6) phase,[35] which appears for an annealing temperature of $T\approx600$ °C. There are, however, some striking differences between these two phases. The "pseudo" (4×6)

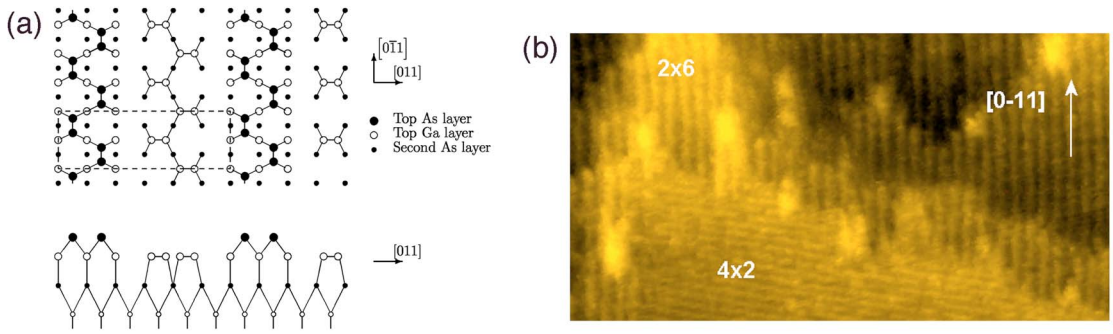

FIG. 2. (Color online) (a) The atomic model for the (2×6) reconstruction as suggested by Biegelsen *et al.* (Ref. 32). The dashed line represents the elementary unit cell of the (2×6) reconstruction. (b) An empty state 50×90 nm^2 STM image of the "pseudo" (4×6) reconstructed GaAs (100) surface. The (2×6) phase (vertical) and the (4×2) phase (horizontal) are clearly distinguishable. The bright spots show disordered Ga clusters surrounding the Ga-rich (4×2) reconstruction. The image was acquired at room temperature with a constant current of 0.5 nA and a sample bias of 1.8 V.

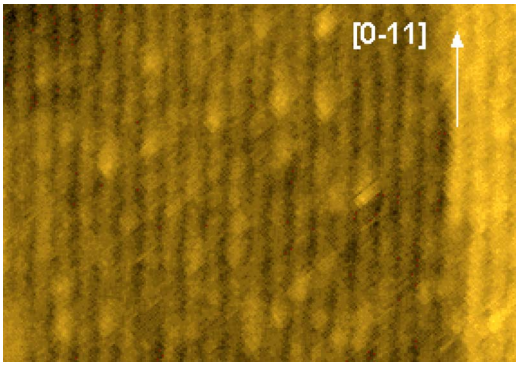

FIG. 3. (Color online) A 33×50 nm^2 STM empty state image of 0.1 ML Fe/GaAs(100)-2×6. The image shows two terraces with the (2×6) reconstruction. The Fe starts to cluster on the top of the As rows. The image was captured with a current of 2.7 nA and a bias of 2.8 V.

is not an intrinsic phase and consists of two different reconstructed domains: the Ga-rich (4×2) and the less Ga-rich (2×6), as shown in Fig. 2(b). The (2×6) was identified to be a transient phase between the As-rich (2×4) and the Ga-rich (4×2) phases. Consequently the (2×6) phase is less Ga-rich compared to the (4×2) due to the As termination. The atomic model for the (2×6) reconstruction, which is presented in Fig. 2(a), was suggested by Biegelsen *et al.*[32]

An empty state STM image of the GaAs surface is displayed in Fig. 2(b). The smaller horizontal phase with the Ga-dimer rows orientated perpendicular to the $[0\bar{1}1]$ axis is the (4×2) phase. It is surrounded by some bright spots that we believe to be disordered regions of Ga clusters as reported by Behrend *et al.*[34] The majority of the images acquired exhibit the (2×6) phase. Therefore, from this point on we will concentrate on this phase. The first layer As-dimer rows of the (2×6) phase are parallel to the $[0\bar{1}1]$ axis. The distance between two rows is 24 Å, compared to an inter-row distance of 16 Å between the Ga-dimer rows of the (4×2) phase. The image reveals five different terraces with four of those having the (2×6) reconstruction while only one exhibits a (4×2) reconstruction. The height difference between two terraces is 1.4 Å corresponding to the separation between neighboring Ga and As planes.[34]

Figure 3 shows an empty state STM image of the lowest coverage studied, nominally 0.1 ML of Fe. The image exhibits two terraces ordered in the (2×6) reconstruction. At this thickness the GaAs surface reconstruction seems to be unmodified. The bright rows observed in the image are associated with the As rows of the (2×6) phase and the deposited Fe molecules appear as bright spots. Relatively large Fe clusters are positioned solely on the top of several As rows. The association of these spots with Fe molecules was determined by multibias imaging in the range from 2.8 to -3.9 V (see discussion below). Furthermore, in their study Wedler *et al.*[37] show that segregation of As and Ga into the Fe film does not occur until the Fe film is at least 2–3 ML thick as indicated by the onset of tensile stress in the film. Their results are in good agreement with those of Lallaizon *et al.*[38] and Kneedler *et al.*,[13] who studied the As and Ga segregation by means of AES and XPS. The islands are typically $\approx$1.4 Å ($\approx$1 ML) high. They have a size of $\approx$24 Å along the $[0\bar{1}1]$ direction (typically covering six As dimers) and $\approx$23 Å along the $[011]$ axis (overreaching the $\approx$8 Å broad As rows). On average, they consist of (35 ± 21) Fe atoms. Furthermore, the (2×6) surface reconstruction remains intact on the sites bordering the Fe clusters. This implies that if any disruption of the surface occurs it is limited to the area underneath the islands.

An STM image taken after 0.3 ML Fe deposition is presented in Fig. 4(a). The image reveals two terraces both exhibiting rows similar to the (2×6) reconstruction in which the As dimers are also visible. The Fe clusters are still predominantly on the top of the As rows, but a few of them have moved on the top of the underlying top Ga dimer layer. In the top right corner on the upper terrace we see already some clusters bridging two As rows. The reconstruction at this stage surrounding the clusters appears to be still intact. We notice that the island density, which is presented in Fig. 7(d), has increased enormously whereas the island size and area has been reduced compared to the 0.1 ML image. The aver-

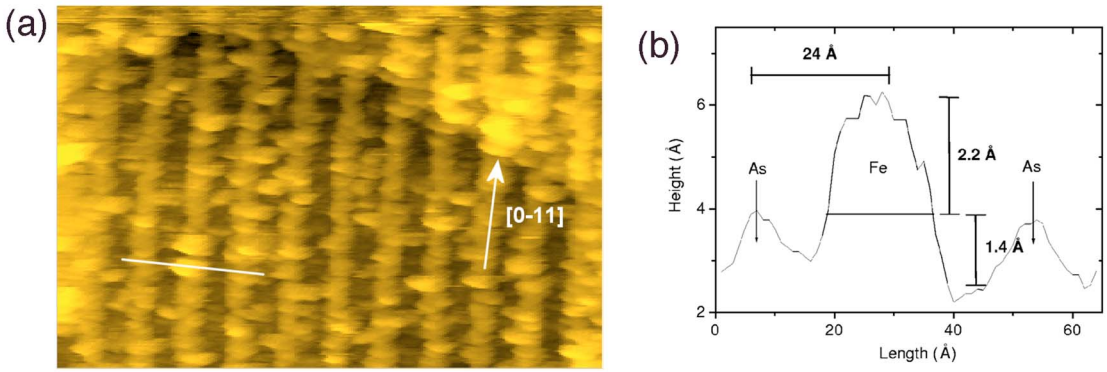

FIG. 4. (Color online) (a) A 16.5×25 nm^2 STM image of 0.3 ML Fe/GaAs(100)-2×6. On the picture two terraces with a (2×6) reconstruction are visible. Most of the Fe islands tend to cluster on the top of the As rows, a few of them are in-between the rows. On the upper terrace on the upper right of the image some clusters have already coalesced and formed a bridge between two rows. The image was captured with a current of 2.6 nA and a bias of 2.8 V. The graph (b) displays the cross-section profile of an Fe cluster which was taken where indicated by the white line in (a).

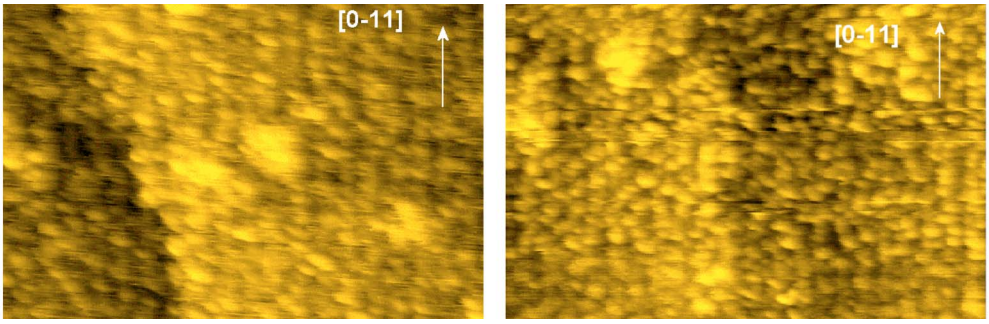

FIG. 5. (Color online) (a) A 33×50 nm^2 empty state STM image of 0.6 ML Fe/GaAs(100)-2×6. On the picture two terraces with a (2×6) reconstruction are visible. A large number of Fe islands are already covering the surface, but the reconstruction is still visible. The image was captured with a current of 1.2 nA and a bias of 1.7 V. (b) A 33×50 nm^2 image of the same coverage which was captured with a current of 2 nA and a bias of −1.1 V.

age island height is now ≈1.5 ML. An elongation of the islands along the [011] direction is visible. These islands consist of (18±11) atoms and have an average size of (10±2) Å along the $[0\bar{1}1]$ direction and (21±4) Å along the [011] axis. Clusters which bridge two As rows are often in a close vicinity to other Fe clusters of approximately the same size or defects in the As row due to a missing dimer. It may be that, lacking enough space to form a desired surface stoichiometry on one row, they impinge on the neighboring row, or that other clusters block their diffusion along the As row. We expect that the diffusion across the Ga rows is easier for three-dimensional (3D) clusters[39–43] than for Fe monomers. Another possible scenario could be that in order to obtain an atomic-scale resolution for this image we have perturbed the small Fe islands with our STM tip from their original position on the top of the As row and moved them above the Ga trenches. This could also explain the islands which are bridging the rows. Figure 4(b) shows a cross-section profile of an Fe cluster in the vicinity of two As rows which was taken where the line indicates it in Fig. 4(a). It should be noticed that the base of the Fe cluster at the height of the underlying As is broader (≈20 Å) than the base of the neighboring As rows (≈15 Å).

Upon doubling the coverage to 0.6 ML as shown in Fig. 5(a), we notice that while the island density per unit area remains almost constant (see Fig. 7), the existing islands grow in size. The height of the islands, however, does not change in-between 0.3–0.6 ML. The As rows are still visible, indicating that the reconstruction next to the islands is not significantly disrupted by the Fe deposition. Some of the Fe islands have already coalesced to form larger clusters. The islands now extend over ≈13 Å along the $[0\bar{1}1]$ direction and ≈23 Å along the [011] axis and consist of (24±16) atoms. As pointed out by Thibado *et al.*,[11] Fe-related features become better distinguishable from the rest of the topography at lower bias [see Figs. 5(a) and 5(b)] due to the property of metal atom clusters on GaAs to create new states in the band gap of semiconductors.[44,45] Figure 5(b) shows a filled state image of the same coverage, but with a lower bias than Fig. 5(a). As mentioned above the Fe clusters can be better distinguished from the underlying GaAs substrate. However, the island sizes and island heights as determined from different bias images [e.g., Figs. 5(a) and 5(b)] do not vary significantly (±10%).

Figure 6 displays the surface after the deposition of 1 ML Fe. Two terraces can be seen, but the surface reconstruction is not observed anymore. However, the regular island arrangement is reminiscent of the initial reconstruction. The average island consists of (53±32) atoms, is ≈21 Å along the $[0\bar{1}1]$ direction and ≈27 Å along the [011] direction and has a height of [(1–2)] ML 2.1±0.4 Å. Some islands have coalesced to form larger clusters but there is no extended percolation visible. Similar results were obtained by Moosbühler *et al.*[14] for the island area of a 1-ML-thick Fe sample, consisting of islands with a height of 1–3 ML which may result from growing on a (4×2) and a (2×6) reconstruction simultaneously. The (4×2) reconstruction is Ga-terminated and therefore an affinity for Fe to bond to Fe instead of Ga on the surface may result in higher clusters for this reconstruction. We also note that we have a surface coverage of ≈50% at this thickness in very good agreement with the previous authors.

IV. DISCUSSION

The island sizes of the Fe clusters for the [011] and $[0\bar{1}1]$ directions vs thickness are presented in Fig. 7(a). Almost circular Fe islands are apparent at 0.1 ML. It is important to note that the small elongation of the islands along the $[0\bar{1}1]$

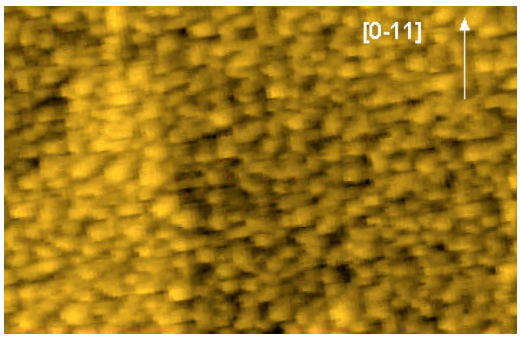

FIG. 6. (Color online) A 33×50 nm^2 STM image of 1.0 ML Fe/GaAs(100)-2×6. The surface is covered by 2D Fe islands. The (2×6) reconstruction can be hardly seen and is only apparent due to the regular island arrangement. The image was acquired with a current of 0.8 nA and a bias of −0.6 V.

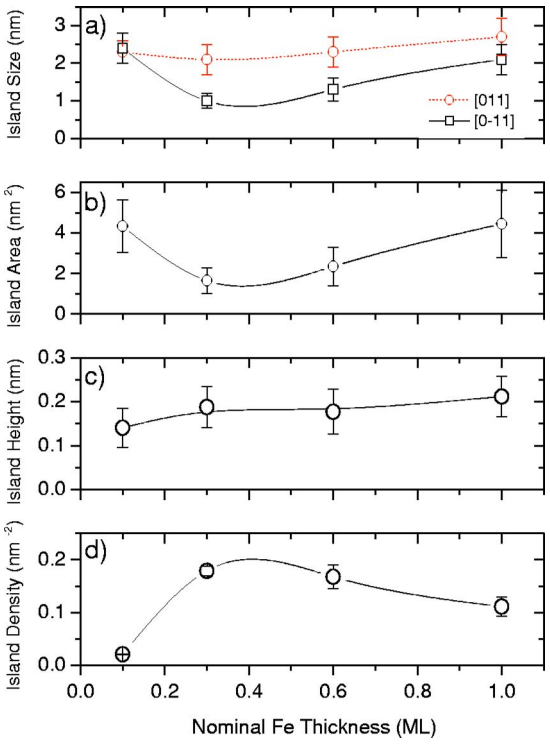

FIG. 7. (Color online) The resulting size (a) and area (b) of the Fe islands during the growth process. The lines are guides to the eye. The height of the Fe islands versus the nominal Fe thickness is presented in (c). At ≈0.4 ML the slope of the height becomes nearly constant. The Fe island density per nm^2 is presented in (d). The island density remains almost constant from 0.3 to 0.6 ML. From this thickness on the coalescence of islands reduces the density by increasing the island size.

direction as reported by other groups for the As rich (2×4) and $c(4\times4)$ phases as determined by STM for the submonolayer regime,[11–13] atomic force microscopy[29] or grazing incidence x-ray diffraction[22] for thicker films is not visible in the submonolayer regime of this study. It is possible that the diffusion along the $[0\bar{1}1]$ direction determines the island shape at this stage, due to a thermodynamic preference for absorption on the free As sites and/or kinetic anisotropies (e.g., faster diffusion along then across the As rows).[11] Our results indicate an almost constant island size along the [011] direction throughout the study while island size changes occur mainly along the $[0\bar{1}1]$ direction. We assume, that in the submonolayer regime, when the As rows are still intact, monomer diffusion along the As rows is highly favorable compared to the direction perpendicular to them where Fe monomers would need to bridge the gap. In addition, from ≈0.4 ML onwards, due to the need to decrease the surface energy of the clusters (rounder clusters being more favorable than strongly elliptical ones), the diffusion along the $[0\bar{1}1]$ direction seems to be more favorable as indicated by the bigger slope for the $[0\bar{1}1]$ direction in Fig. 7(a). This results in some clusters being almost circular at 1 ML, while at intermediate coverages the islands are clearly elliptical. Indeed our STM results for a 2-ML-thick film (not shown here)[46] indicate an elongation of the Fe islands along the $[0\bar{1}1]$ direction in agreement with other studies of thicker films.[22,29] The decrease in island size from 0.1 to 0.3 ML is accompanied by an increase in island height [Fig. 7(c)] and island density [Fig. 7(d)]. At 0.3 ML, the relatively small variance in island size and area [Figs. 7(a) and 7(b)] as compared to the other coverages studied indicates relatively stable Fe clusters for these growth parameters. The larger error bars for the other thicknesses arise mainly from the statistical distribution of island sizes for these coverages but also from the difficulty of distinguishing between the area of the SC and Fe clusters from the results of the 2D height-height autocorrelation function for the 1 ML coverage. Figure 7(b) shows that after a decrease in island area from 0.1 to 0.3 ML upon increasing the Fe coverage from 0.3 to 1.0 ML the area of the islands increases monotonically. As shown in Fig. 7(c) between 0.1 to 0.3 ML significant changes in the island height occur. From 0.3 ML on, the island height remains fairly constant. Our results indicate a transition from a 3D cluster growth mode at 0.3 ML towards a 2D island nucleation between 0.3 and 1 ML, as reported for Fe growth on the As-rich (2×4) reconstruction for coverages ⩽3 ML in Refs. 11 and 12. Moreover, other studies also indicate an initial 3D Volmer-Weber growth mode[16,18,19,27–29] followed by a gradual smoothening at different thicknesses possibly depending on the surface reconstruction. Assuming that the Fe adatoms on the top of the Fe islands have a constant mobility, then on smaller islands they visit the edge more frequently than on large islands. Therefore, the attempt frequency of adatoms descending the island edge is increased and in addition the interlayer diffusion barrier (Schwoebel barrier[47]) is likely to be lowered because of the smaller island size.[48] This would result in an enhanced Fe interlayer diffusion from 0.3 to 1 ML.[49] The island density vs thickness is displayed in Fig. 7(d), where we can determine three steps in the growth mode. First from 0.1 to 0.3 ML the system is in the nucleation regime in which the density of islands increases. Then it is followed by the island growth regime (intermediate-coverage regime) when the island density remains constant from 0.3 to 0.6 ML while the single islands grow in size. From 0.6 ML the system is in the coalescence regime where islands, due to their size or cluster diffusion start to undergo fusion. The last regime of structural percolation of the islands, as indicated by the onset of ferromagnetism, is reported to occur either at ≈2.5 ML (Ref. 19) (0 K) or at ≈3.6 ML (RT) as given by Refs. 19 and 21 and therefore lies outside our studied thickness range.

From the island densities and volumes measured we have determined the real atomic coverage of our substrate assuming bcc Fe spacing[11,14] and semi-ellipsoidal Fe islands (even though the islands are seldom symmetrical as can be seen from the images). This we have compared to the nominal thickness of deposited Fe. The results are displayed in Fig. 8. At 0.1 ML the deviation can be described as a result of the difference in Fe atom spacing in the film compared to bcc Fe or a slight miscalibration of the Fe evaporator. For thicknesses greater than 0.3 ML, the difference between real and nominal thickness becomes more pronounced indicating Fe atom loss. The Fe atoms have an affinity to bond to As even more than to other Fe atoms and are also looking for a po-

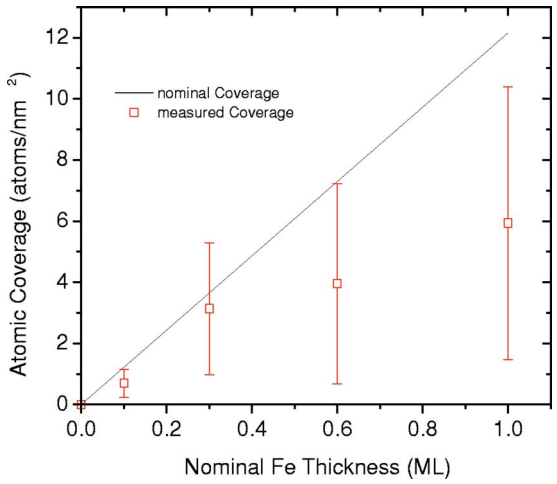

FIG. 8. (Color online) The difference between nominal and real atomic coverage. The discrepancy can neither be explained by the error calculation nor by an assumed miscalibration of the evaporation source. Therefore a reasonable assumption is that Fe adatoms diffuse into the substrate as proposed and calculated by Erwin *et al.* (Ref. 50) and Mirbt *et al.* (Ref. 51).

sition with a high coordination number.[50,51] We propose that Fe penetrates into the top As layer of the GaAs surface and additionally substitutes the Ga on the second layer displacing it into an interstitial position.

Based on our analysis, we suggest a structural model for the nucleation sites in the submonolayer regime of Fe growth on GaAs(100)-2×6, consisting at 0.3 ML mostly of twenty-atom islands. The Fe atoms are atop of the first-layer As rows and inside the first As layer. The islands are separated along each row at least by a single missing As dimer. However, we speculate that the As dimers inside the islands are broken in favor of FeAs bonds. The broader base underneath the Fe islands as compared to the unperturbed As dimers [Fig. 4(b)] indicates that a chemical reaction accompanied by a rearrangement of the atoms may have occurred. However, for energetic reasons, after the cluster has diffused along a row, the broken As and Ga dimers are reformed in order to reduce the number of dangling bonds[35] so that the vicinity of the clusters seems to be unperturbed. The vicinity of As atoms should be energetically more favorable for an Fe atom than a position atop of the island due to the affinity of Fe for a high coordination number. A top view of the proposed structural model for the stable Fe islands at 0.3 ML is presented in Fig. 9(a). Figure 9(b) presents the suggested substitutional position of Fe atoms inside the second layer with the Ga displaced into an interstitial position.

Figure 10(a) shows a 3D image from the top onto our modelled islands and their environment at a nominal thickness of 0.3 ML, while Fig. 10(b) represents a side view of such an island. Fe atoms are shown in bright gray (gray), As atoms in gray (cyan), and Ga atoms in dark gray (blue), respectively.

The islands at 0.3 ML are as already mentioned already relatively stable, possibly due to the fact that they have an optimal surface stoichiometry. The visible eighteen Fe atoms in the clusters, the four As atoms underneath and the four As atoms in the close vicinity would leave us with a surface

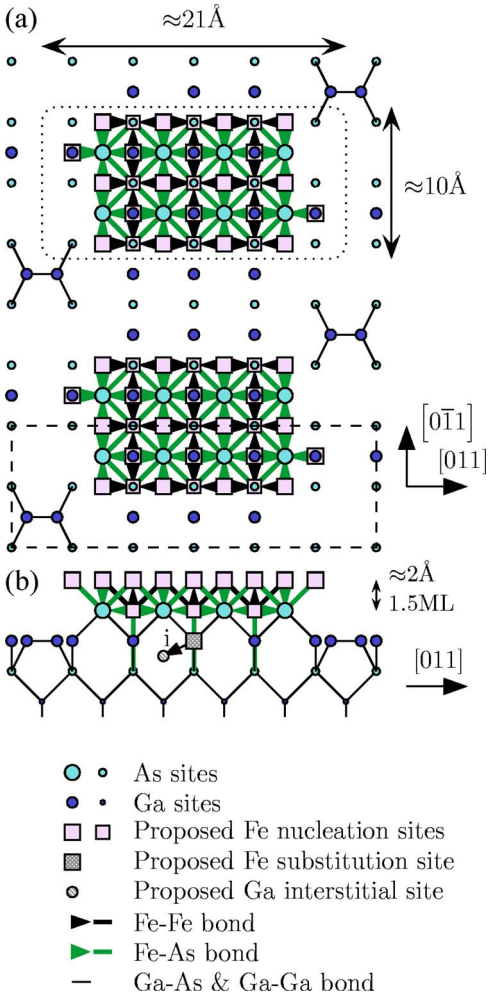

FIG. 9. (Color online) (a) Top view of our proposed structural model for the Fe island nucleation observed for 0.3 ML. The dashed line represents the elementary unit cell of the initial (2×6) reconstruction. The dotted line shows the boundary of the average cluster. Triangular bonds inside the clusters indicate an out of plane bonding, whereas thick lines represent in-plane bonds in the model. It is assumed that the adsorbed Fe atoms are inside and 1 ML above the top As layer. The islands are always separated along the [0$\bar{1}$1] direction by at least one missing As dimer. The bottom image (b) displays a side view of our model with Fe substituting on Ga sites and Ga on an interstitial position (i).

stoichiometry of $Fe_{2.25}As$, close to the stoichiometric compound Fe_2As. Fe_2As seems to be a perfectly suitable candidate as a template for Fe growth on GaAs(100) and therefore we suggest that the antiferromagnetic Fe_2As acts as the "seed" crystals which nucleate the subsequent bcc Fe growth. Fe_2As grains have been already reported for high-temperature grown[52] and post growth annealed Fe films[53–55] as observed by x-ray diffraction. Fe_2As crystallizes in the tetragonal Cu_2Sb ($P4/nmm$) structure with the lattice parameters $a=3.627$ Å and $c=5.981$ Å (Fig. 11). It possesses two nonequivalent Fe sites with two different magnetic moments.[56] The epitaxial relationship of the planes in our model and for the following bcc Fe growth is (100)GaAs‖(100)Fe_2As‖(100)Fe and this within the plane [011]GaAs‖[001]Fe_2As‖[011]Fe. We are aware that this is

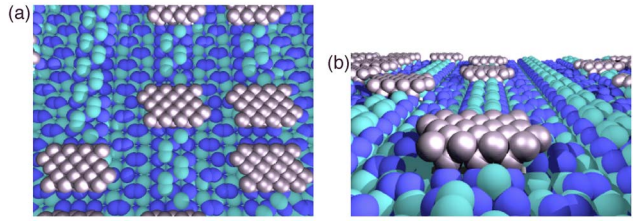

FIG. 10. (Color online.) (a) A 3D topview of our suggested modelled island and environment at a nominal Fe coverage of 0.3 ML. (b) A 3D side-view of our modelled island.

in contrast to the epitaxial relation determined for post-annealed samples $[111](100)GaAs \| [101](011)Fe_2As$.[52,54,55] Also from strain considerations the latter relation seems slightly better than ours. However, the large distance between adjacent Fe chains on the (011) Fe_2As plane (5.981 Å) is too big for the following bcc Fe growth and neither can we detect such large gaps in our clusters. Therefore, the (100) Fe_2As plane seems more feasible for the following bcc Fe growth. Furthermore, by inspecting the high-resolution transmission electron microscopy images from Monteverde *et al.*[55], our suggested epitaxial relation is partially also visible at the bottom of their trapezoidal Fe_2As grains.

However, Fe_2As alone cannot account for all the missing Fe atoms but for only 0.2 ML of Fe, taking into account that only 50% of the surface is covered at the nominal coverage of 1 ML. From a "naive" point of view we can say that the islands want to maintain the Fe_2As surface composition. Therefore excess Fe atoms searching for a high coordination number penetrate into the substrate and substitute for Ga, while Ga remains interstitial as shown in Fig. 9(b). The resulting formation energy, which is released due to this mechanism can be transfered to adatoms of Fe on the top of the islands to surmount the Schwoebel barrier even for larger islands, for which the edge visiting frequency decreases. This would explain the increased smoothening of the island surfaces towards a 2D island nucleation, which has been observed in our study and by other groups for the growth on the (2×4) and the "pseudo" (4×6) reconstructed surfaces.[12,27] We speculate as stated by Rosenfeld *et al.*[49] that as island sizes increase due to coalescence it gets more and more difficult for adatoms to surmount the Schwoebel barrier and from 1.5–3 ML the system may undergo a second transition to 3D cluster growth (Volmer-Weber growth). It should be mentioned that upon further deposition the substitutional position of Fe and the interstitial position of Ga is not energetically favorable.[50] This could lead to an outdiffusion of the Fe from the substrate followed by a segregation of As and Ga into the Fe film.[13,37] This intermixing would destroy the substrate reconstruction leaving behind randomly distributed Fe, As, and Ga atoms at the interface[37] in contrast to the high-temperature growth where the presence of $Fe_2Ga_{2-x}As_x$ has been reported. Calculating all possible positions for Fe inside the first GaAs layers results in a capacity of 0.2 ML [see position (i) shown in Fig. 9(b)] upon substitution into the interstitial position and up to 0.4 ML (Fig. 9) if we add the Fe atoms inside the first As layer, which form part of the Fe_2As "seed" crystal. These positions can account for the missing 0.2–0.5 ML Fe at a thickness of nominally 1 ML. Support for our model can also be found in the stress evolution study of Wedler *et al.*[37] They have used substrates prepared almost exactly in the same way as in the present study and upon Fe deposition they measure the film stress. The submonolayer region exhibits only a compressive stress, which is significantly larger than the value of the maximum possible misfit stress. This supports our model in which smaller Fe atoms substitute for Ga in the zinc blende structure. Similarly Gustavsson *et al.*,[57] who have studied the growth of Fe on the Zn-terminated $c(2\times2)$ reconstructed ZnSe surface, suggest that Fe atoms are embedded inside the top Zn layer favoring bonding to the underlying Se layer. It is important to note that as shown in our model, the Fe_2As "seed" crystal possesses Fe-Fe bonds, e.g., Fe in the next neighbor vicinity of Fe leading to a non-zero magnetic moment on the two crystallographically nonequivalent Fe sites. Recently the results of x-ray magnetic circular dichroism spectroscopy measurements by Claydon *et al.*[58] on our samples as well as by Giovanelli *et al.*[59] rule out the existence of magnetically "dead" layers and indicate even for the submonolayer region the existence of a magnetic phase at the interface. A clear understanding of the chemical composition at the Fe/GaAs interface, however, requires a study of the submonolayer regime by using atomic resolution transmission electron microscopy.

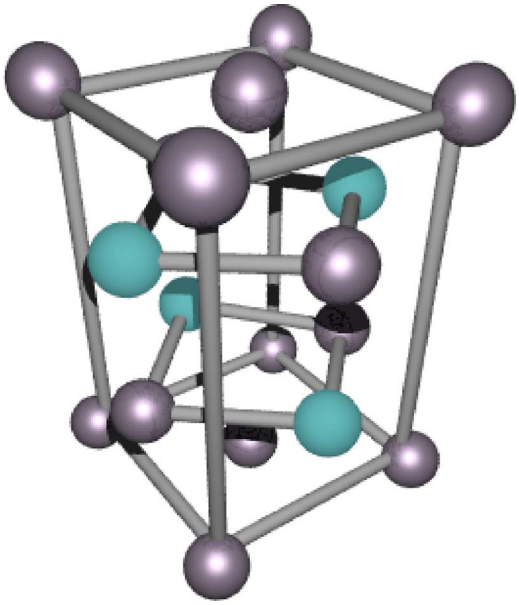

FIG. 11. (Color online.) The tetragonal structure of Fe_2As with dark gray (gray) spheres representing Fe and light gray (cyan) ones As.

V. CONCLUSIONS

We have used STM to study the submonolayer growth of Fe on $GaAs(100)-2\times6$, which is a Ga-rich and As terminated surface. We show that the growth of Fe clusters in the early nucleation stage around 0.1 ML solely occurs atop the As-dimer rows. The clusters exhibit at this thickness an almost circular shape. Throughout our study the island sizes

along the [011] direction do not vary much in contrast to the situation along the $[0\bar{1}1]$ direction indicating that Fe atom diffusion occurs mainly along the As rows. In the nucleation regime, at 0.3 ML the cluster sizes of individual islands do not vary much as compared to the other coverages studied. In this regime, a transition from the 3D cluster growth to a 2D island nucleation takes place due to the high visiting frequency of the edge by the Fe adatoms atop the Fe islands due to the reduced island sizes at 0.3 ML. Upon further Fe deposition from 0.3 to 0.6 ML the system changes into the growth regime as indicated by a constant island density and increasing island sizes. At 1 ML the coalescence of several islands leads to a large distribution of island sizes and a decreased island density. Throughout our study from 0.3 ML onwards we observe an Fe atom loss in our surface coverage, which becomes more distinct at higher coverages, suggesting penetration of Fe into the GaAs substrate. Based on our results we propose a structural model for the initial nucleation at 0.3 ML. Therein Fe atoms substitute for Ga atoms in the second layer displacing them into an interstitial position. In addition, Fe inside the top As layer together with the top Fe layer forms Fe_2As "seed" crystals for the bcc Fe growth.

ACKNOWLEDGMENTS

M.T. gratefully acknowledges the financial support of EC (TMR: "SUBMAGDEV"). D.M.G. expresses his gratitude to EPSRC for their funding. S.J.S thanks EPSRC and ABB (Sweden) for the financial support. G.W. is grateful for the financial support of the Austrian Academy of Sciences, the Wilhelm-Macke-Stipendienprivatstiftung (Austria), the Cambridge Philosophical Society (UK), the Lundgren Fund (UK) and Selwyn College, Cambridge (UK). A.I. thanks the Cambridge European Trust and Nordiko, Ltd. for their funding.

*Corresponding author. Electronic address: jacb1@phy.cam.ac.uk

[1] J. R. Waldrop and R. W. Grant, Appl. Phys. Lett. **34**, 630 (1979).
[2] R. Fiederling, M. Keim, G. Reuscher, W. Ossau, G. Schmidt, A. Waag, and L. W. Molenkamp, Nature (London) **402**, 787 (1999).
[3] Y. Ohno, D. K. Young, B. Beschoten, F. Matsukura, H. Ohno, and D. D. Awschalom, Nature (London) **402**, 790 (1999).
[4] S. Datta and B. Das, Appl. Phys. Lett. **56**, 665 (1989).
[5] M. Johnson, Phys. Rev. B **58**, 9635 (1998).
[6] G. A. Prinz, Science **250**, 1092 (1990).
[7] G. A. Prinz, Science **282**, 1660 (1998).
[8] G. Schmidt, D. Ferrand, L. W. Molenkamp, A. T. Filip, and B. J. van Wees, Phys. Rev. B **62**, R4790 (2000).
[9] G. Schmidt and L. W. Molenkamp, Semicond. Sci. Technol. **17**, 310 (2002).
[10] E. I. Rashba, Phys. Rev. B **62**, R16 267 (2000).
[11] P. M. Thibado, E. Kneedler, B. T. Jonker, B. R. Bennett, B. V. Shanabrook, and L. J. Whitman, Phys. Rev. B **53**, R10481 (1996).
[12] E. Kneedler, P. M. Thibado, B. T. Jonker, B. R. Bennett, B. V. Shanabrook, R. J. Wagner, and L. J. Whitman, J. Vac. Sci. Technol. B **14**, 3193 (1996).
[13] E. M. Kneedler, B. T. Jonker, P. M. Thibado, R. J. Wagner, B. V. Shanabrook, and L. J. Whitman, Phys. Rev. B **56**, 8163 (1997).
[14] R. Moosbühler, F. Bensch, M. Dumm, and G. Bayreuther, J. Appl. Phys. **91**, 8757 (2002).
[15] J. J. Krebs, B. T. Jonker, and G. A. Prinz, J. Appl. Phys. **61**, 2569 (1987).
[16] Y. B. Xu, E. T. M. Kernohan, D. J. Freeland, A. Ercole, M. Tselepi, and J. A. C. Bland, Phys. Rev. B **58**, 890 (1998).
[17] Y. B. Xu, E. T. M. Kernohan, D. J. Freeland, M. Tselepi, A. Ercole, and J. A. C. Bland, J. Magn. Magn. Mater. **198**, 703 (1999).
[18] M. Brockmann, M. Zölfl, S. Miethaner, and G. Bayreuther, J. Magn. Magn. Mater. **198**, 384 (1999).
[19] F. Bensch, G. Garreau, R. Moosbühler, G. Bayreuther, and E. Beaurepaire, J. Appl. Phys. **89**, 7133 (2001).
[20] F. Bensch, Ph.D. thesis, Universität Regensburg, 2001.
[21] S. J. Steinmüller, M. Tselepi, G. Wastlbauer, V. Strom, D. M. Gillingham, A. Ionescu, and J. A. C. Bland , Phys. Rev. B **70**, 024420 (2004).
[22] O. Thomas, Q. Shen, P. Schieffer, N. Tournerie, and B. Lépine, Phys. Rev. Lett. **90**, 017205 (2003).
[23] G. Wastlbauer, Ph.D. thesis, University of Cambridge, 2004.
[24] G. Wastlbauer and J. A. C. Bland, Adv. Phys. **54**, 137 (2005).
[25] M. Gester, C. Daboo, R. J. Hicken, S. J. Gray, A. Ercole, and J. A. C. Bland, J. Appl. Phys. **80**, 347 (1996).
[26] J. W. Freeland, I. Coulthard, W. J. Antel, Jr., and A. P. J. Stampfl, Phys. Rev. B **63**, 193301 (2001).
[27] M. Gester, C. Daboo, S. J. Gray, and J. A. C. Bland, J. Magn. Magn. Mater. **165**, 242 (1997).
[28] S. A. Chambers, F. Xu, H. W. Chen, I. M. Vitomirov, S. B. Anderson, and J. H. Weaver, Phys. Rev. B **34**, 6605 (1986).
[29] Y. Chye, V. Huard, M. E. White, and P. M. Petroff, Appl. Phys. Lett. **80**, 449 (2002).
[30] M. Zölfl, M. Brockmann, M. Köhler, S. Kreuzer, T. Schweinböck, S. Miethaner, F. Bensch, and G. Bayreuther, J. Magn. Magn. Mater. **175**, 16 (1997).
[31] R. A. Gordon, E. D. Crozier, D. T. Jiang, T. L. Monchesky, and B. Heinrich, Phys. Rev. B **62**, 2151 (2000).
[32] D. K. Biegelsen, R. D. Bringans, J. E. Northrup, and L. E. Swartz, Phys. Rev. B **41**, 5701 (1990).
[33] Q. Xue, T. Hashizume, J. M. Zhou, T. Sakata, T. Ohno, and T. Sakurai, Phys. Rev. Lett. **74**, 3177 (1995).
[34] J. Behrend, M. Wassermeier, L. Däweritz, and K. H. Ploog, Surf. Sci. **342**, 63 (1995).
[35] Q. Xue, T. Hashizume, and T. Sakurai, Appl. Surf. Sci. **141**, 244 (1999).
[36] H. Xu, Y. G. Li, A. T. S. Wee, C. H. A. Huan, and E. S. Tok, Surf. Sci. **513**, 249 (2002).
[37] G. Wedler, B. Wassermann, R. Nötzel, and R. Koch, Appl. Phys. Lett. **78**, 1270 (2001).
[38] C. Lallaizon, B. Lépine, S. Ababou, A. Guivarc'h, S. Députier, F. Abel, and C. Cohen, J. Appl. Phys. **86**, 5515 (1999).
[39] J. M. Soler, Phys. Rev. B **53**, R10540 (1996).
[40] J. M. Wen, S. L. Chang, J. W. Burnett, J. W. Evans, and P. A.

Thiel, Phys. Rev. Lett. **73**, 2591 (1994).
[41] J. M. Wen, J. W. Evans, M. C. Bartelt, J. W. Burnett, and P. A. Thiel, Phys. Rev. Lett. **76**, 652 (1996).
[42] A. Masson, J. J. Métois, and R. Kern, Surf. Sci. **27**, 463 (1971).
[43] R. Kern, A. Masson, and J. J. Métois, Surf. Sci. **27**, 483 (1971).
[44] P. N. First, J. A. Stroscio, R. A. Dragoset, D. T. Pierce, and R. J. Celotta, Phys. Rev. Lett. **63**, 1416 (1989).
[45] R. M. Feenstra, Appl. Surf. Sci. **56–58**, 104 (1992).
[46] D. M. Gillingham, M. Tselepi, A. Ionescu, and J. A. C. Bland (unpublished).
[47] R. L. Schwoebel, J. Appl. Phys. **40**, 614 (1968).
[48] N. Memmel and E. Bertel, Phys. Rev. Lett. **75**, 485 (1995).
[49] G. Rosenfeld, R. Servaty, C. Teichert, B. Poelsema, and G. Comsa, Phys. Rev. Lett. **71**, 895 (1993).
[50] S. C. Erwin, S. H. Lee, and M. Scheffler, Phys. Rev. B **65**, 205422 (2001).
[51] S. Mirbt, B. Sanyal, C. Isheden, and B. Johansson, Phys. Rev. B **67**, 155421 (2003).
[52] H. P. Schönherr, R. Nötzel, W. Ma, and K. H. Ploog, J. Appl. Phys. **89**, 169 (2001).
[53] S. Députier, R. Guérin, and A. Guivarc'h, Eur. Phys. J. A **2**, 127 (1998).
[54] B. Lépine, S. Ababou, A. Guivarc'h, G. Jézéquel, S. Députier, R. Guérin, A. Filipe, A. Schuhl, F. Abel, C. Cohen, A. Rocher, and J. Crestou, J. Appl. Phys. **83**, 3077 (1998).
[55] F. Monteverde, A. Michel, J. P. Eymery, and J. C. Desoyer, Appl. Surf. Sci. **172**, 265 (2001).
[56] P. Raj and S. K. Kulshreshtha, Phys. Scr. **14**, 125 (1976).
[57] F. Gustavsson, E. Nordström, V. H. Etgens, M. Eddrief, E. Sjöstedt, R. Wäppling, and J. M. George, Phys. Rev. B **66**, 024405 (2002).
[58] J. S. Claydon, Y. B. Xu, M. Tselepi, J. A. C. Bland, and G. van der Laan, Phys. Rev. Lett. **93**, 037206 (2004).
[59] L. Giovanelli, C. S. Tian, P. L. Gastelois, G. Panaccione, M. Fabrizioli, M. Hochstrasser, M. Galaktionov, C. H. Back, and G. Rossi, Physica B **345**, 177 (2004).